Asynchronous Multi-Radar Tracking Fusion with Converted Measurements

Donglin Zhang, Zhansheng Duan
Center for Information Engineering Science Research
Xi'an Jiaotong University
Xi'an, Shaanxi 710049, China
Email: zdlin23@stu.xjtu.edu.cn, zsduan@mail.xjtu.edu.cn

Uwe D. Hanebeck
Intelligent Sensor-Actuator-Systems Laboratory (ISAS)
Institute for Anthropomatics and Robotics
Karlsruhe Institute of Technology (KIT), Germany
Email: uwe.hanebeck@kit.edu

***Abstract*—In tracking applications, multiple radars used to observe target motion usually work asynchronously due to different sampling rates and initial sampling time instants, and the fusion time instant at the fusion center can be designated arbitrarily. In this paper, the estimation fusion problem for target tracking with asynchronous multi-rate multi-radar measurements is investigated. Two asynchronous fusion algorithms are proposed, i.e., batch time-aligned asynchronous fusion with unbiased converted measurements and sequential linear minimum mean square error (LMMSE) asynchronous fusion with converted measurements. The batch time-aligned asynchronous fusion algorithm is suboptimal because of the correlation between measurement error covariance and measurement itself. The sequential LMMSE asynchronous fusion algorithm is theoretically optimal in the sense of minimizing the mean square error within the set of all linear estimators. Numerical examples are provided to demonstrate the effectiveness of the proposed two asynchronous fusion algorithms.**

***Index Terms*—Asynchronous fusion, multi-radar measurements, LMMSE, measurement conversion, target tracking.**

I. Introduction

The problem of target tracking with radar measurements has been of great interest for various civilian and military applications, e.g., intelligent traffic monitoring, anti-missile system, and air traffic control and battlefield surveillance [1, 2]. In tracking applications, multiple radars observe target state in the original sensor coordinates, while the fusion center commonly performs tracking in the Cartesian coordinates. Due to the nonlinear relationship between the polar/spherical coordinates and Cartesian coordinates, tracking in Cartesian coordinates using raw radar measurements is essentially a nonlinear filtering problem. Therefore, the regular nonlinear filters, e.g., extended Kalman filter (EKF) [3], unscented Kalman filter (UKF) [4], divided difference filter (DDF) [5], quadrature Kalman filter (QKF) [6], and particle filter (PF) [7], can be used by simply stacking all raw radar measurements up.

To circumvent the limitations of these regular nonlinear filters for target tracking, such as high computational complexity and suboptimal estimation accuracy, a specially designed nonlinear filtering approach is commonly employed to address the problem of tracking with radar measurements in polar/spherical coordinates. The converted measurement Kalman filter (CMKF) converts the polar/spherical radar measurement model into a pseudolinear form in Cartesian coordinates, allowing for the use of the standard Kalman filter. Existing approaches for measurement conversion include the debiased converted measurement (DCM) [8], unbiased converted measurement (UCM) [9], modified unbiased converted measurement (MUCM) [10], decorrelated unbiased converted measurement (DUCM) [11], and the unscented transformation (UT) [12].

An optimal LMMSE filter for target tracking was proposed in [13], which minimizes the mean square error among all linear unbiased estimators. In this filter, the moments needed in filtering are computed as accurately as possible by using the converted measurements. For the synchronous multi-radar case, the existing LMMSE filter has been extended by simply stacking all converted measurements up [14]. To improve the performance of the LMMSE centralized fusion, recombination and compression approaches for multi-radar measurements were applied [14, 15]. To reduce the computational complexity, we further proposed a recursive LMMSE sequential fusion algorithm in [16] and proved that it is equivalent to the LMMSE centralized fusion algorithm.

In practice, the target motion is observed by an arbitrary number of radars with different sampling rates and initial sampling time instants, and the fusion time instant at the fusion center can be designated arbitrarily as well [17, 18]. In [19], a decentralized asynchronous track-to-track fusion algorithm was proposed for target tracking in asynchronous two-dimensional radar networks. This algorithm is not optimal due to the approximation about the measurement conversion from polar to Cartesian coordinates. Since multiple radars work asynchronously, the original LMMSE fusion algorithms are not applicable. In this paper, we will extend the LMMSE fusion to the tracking cases with asynchronous multi-rate multi-radar measurements. By aligning measurements collected at different time instants to a common fusion time instant or constructing a state-transition model to the measurement time instant, two asynchronous fusion algorithms are proposed using measurement conversion. The proposed sequential

This work is supported in part by National Key Research and Development Plan under Grants 2021YFC2202600 and 2021YFC2202603, and National Natural Science Foundation of China through Grants 62033010, 61773147 and 61673317.

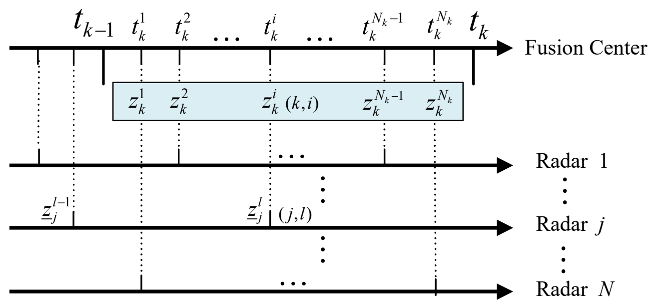

Fig. 1: Radar measurements during time interval $(t_{k-1}, t_k]$.

LMMSE asynchronous fusion with converted measurements is the best within the set of all linear estimators.

This paper is organized as follows. Section II formulates the problem. Section III presents batch time-aligned asynchronous fusion with unbiased converted measurements and sequential LMMSE asynchronous fusion with converted measurements. Section IV provides illustrative examples to verify the performance of the proposed two asynchronous fusion algorithms. Section V gives conclusions.

II. Problem Formulation

Consider the following motion model of a target to be tracked described by a continuous-time linear stochastic differential equation

$$\dot{\boldsymbol{x}}(t) = \boldsymbol{A}(t)\boldsymbol{x}(t) + \boldsymbol{D}(t)\widetilde{\boldsymbol{w}}(t), \tag{1}$$

where $\boldsymbol{x}(t) = [x(t), \dot{x}(t), y(t), \dot{y}(t)]^T$ is the target state vector in two-dimensional Cartesian coordinates, $\boldsymbol{A}(t)$ and $\boldsymbol{D}(t)$ are known coefficient matrices with appropriate dimensions, $\widetilde{\boldsymbol{w}}(t)$ is continuous-time zero-mean white process noise with power spectral density $\tilde{\boldsymbol{q}}(t)$.

Let t_k, $k \in \mathbb{N}$, be the time instant when the fusion center executes the current tracking fusion operation. The target motion is observed by N radars with different initial sampling time instants and sampling periods. Suppose that a total number of N_k measurements are collected by all these N radars during time interval $(t_{k-1}, t_k]$. As shown in Fig. 1, these N_k measurements collected asynchronously can be arranged in time sequence, where $\boldsymbol{z}_k^i$ is the i-th measurement in $(t_{k-1}, t_k]$. Denoting t_k^i as the time instant when $\boldsymbol{z}_k^i$ is collected, we have $t_{k-1} < t_k^1 \leq t_k^2 \leq \cdots \leq t_k^{N_k} \leq t_k$, where the equalities hold when two associated measurements are obtained at the same time.

During the time interval $(t_{k-1}, t_k]$, a radar may have provided more than one measurement because these radars are multi-rate and asynchronous, or perhaps it has provided no measurement at all. Denote by n_k^j the number of measurements provided by radar j. Then we have

$$N_k = \sum_{j=1}^{N} n_k^j. \tag{2}$$

As shown in Fig. 1, a unique one-to-one correspondence between (k,i) and (j,l), $k \in \mathbb{N}$, $i \in \{1, \cdots, N_k\}$, $j \in \{1, \cdots, N\}$, $l \in \mathbb{N}$, can be determined to represent that the i-th measurement $\boldsymbol{z}_k^i$ during the k-th time interval $(t_{k-1}, t_k]$ is the l-th measurement $\underline{\boldsymbol{z}}_j^l$ provided by radar j at time t_k^i, that is, $\boldsymbol{z}_k^i = \underline{\boldsymbol{z}}_j^l$.

Let $\boldsymbol{z}_k^i = [r_k^{m_i}, b_k^{m_i}]^T$. Then the radar measurements, range $r_k^{m_i}$ and bearing (or azimuth) $b_k^{m_i}$ in polar coordinates at time t_k^i, are defined as

$$\begin{aligned} r_k^{m_i} &= r_k^i + \tilde{r}_k^i, \\ b_k^{m_i} &= b_k^i + \tilde{b}_k^i, \end{aligned} \tag{3}$$

where

$$\begin{aligned} r_k^i &= \sqrt{(x(t_k^i))^2 + (y(t_k^i))^2}, \\ b_k^i &= \tan^{-1}\left(y(t_k^i)/x(t_k^i)\right) \end{aligned} \tag{4}$$

are the corresponding ground truth, $\tilde{r}_k^i$ and $\tilde{b}_k^i$ are zero-mean white measurement noises with standard deviation σ_r^i and σ_b^i, respectively. We assume that they are uncorrelated with each other and uncorrelated with $\boldsymbol{x}(0)$ and $\widetilde{\boldsymbol{w}}(t)$, and independent across radars. For convenience, all radars used to observe the target state are assumed to be co-located at the origin of the Cartesian coordinates where target dynamics are modeled.

III. Asynchronous Fusion with Converted Measurements

Denote $\Phi(t_k, t_{k-1})$ as the state transition matrix from time t_{k-1} to t_k, and T_f as the sampling period of fusion center. Discretizing the continuous-time linear system (1), the corresponding discrete-time dynamic model of the target is then obtained as

$$\boldsymbol{x}(t_k) = \Phi(t_k, t_{k-1})\boldsymbol{x}(t_{k-1}) + \boldsymbol{w}(t_k, t_{k-1}), \tag{5}$$

where

$$\begin{aligned} t_k &= kT_f, \ k \in \mathbb{N}, \\ \boldsymbol{w}(t_k, t_{k-1}) &= \int_{t_{k-1}}^{t_k} \Phi(t_k, \tau)\boldsymbol{D}(\tau)\widetilde{\boldsymbol{w}}(\tau)d\tau. \end{aligned} \tag{6}$$

Under the zero-mean and white noise assumptions on $\widetilde{\boldsymbol{w}}(t)$ in (1), it follows that

$$\begin{aligned} E[\boldsymbol{w}(t_k, t_{k-1})] &= 0, \\ E[\boldsymbol{w}(t_k, t_{k-1})\boldsymbol{w}^T(t_l, t_{l-1})] &= \boldsymbol{Q}(t_k, t_{k-1})\delta_{kl}, \end{aligned} \tag{7}$$

where δ_{kl} is the Kronecker delta function. Then the covariance of the discrete-time process noise $\boldsymbol{w}(t_k, t_{k-1})$ is given by

$$\boldsymbol{Q}(t_k, t_{k-1}) = \int_{t_{k-1}}^{t_k} \Phi(t_k, \tau)\boldsymbol{D}(\tau)\tilde{\boldsymbol{q}}(\tau)\boldsymbol{D}^T(\tau)\Phi^T(t_k, \tau)d\tau. \tag{8}$$

For convenience, we define

$$\begin{cases} \lambda_1^i = E[\cos\tilde{b}_k^i] = e^{-(\sigma_b^i)^2/2} \\ \lambda_2^i = E[\cos^2\tilde{b}_k^i] = (1 + e^{-2(\sigma_b^i)^2})/2 \\ \lambda_3^i = E[\sin^2\tilde{b}_k^i] = (1 - e^{-2(\sigma_b^i)^2})/2 \\ \lambda_4^i = E[\cos 2\tilde{b}_k^i] = e^{-2(\sigma_b^i)^2} \end{cases}. \tag{9}$$

A. Batch Time-Aligned Asynchronous Fusion with Unbiased Converted Measurements

Given the true range r_k^i and bearing b_k^i, the unbiased measurement conversion with multiplicative debiasing at time t_k^i is [9]

$$\begin{aligned} x_k^{u_i} &= (\lambda_1^i)^{-1} r_k^{m_i} \cos b_k^{m_i}, \\ y_k^{u_i} &= (\lambda_1^i)^{-1} r_k^{m_i} \sin b_k^{m_i}. \end{aligned} \tag{10}$$

Let $\boldsymbol{y}_k^{u_i} = [x_k^{u_i}, y_k^{u_i}]^T, i = 1, \cdots, N_k$, and

$$\boldsymbol{H}_k^i = \begin{bmatrix} 1 & 0 & 0 & 0 \\ 0 & 0 & 1 & 0 \end{bmatrix}. \tag{11}$$

Then the unbiased converted measurements at time t_k^i can be compactly rewritten as

$$\boldsymbol{y}_k^{u_i} = \boldsymbol{H}_k^i \boldsymbol{x}(t_k^i) + \boldsymbol{v}_k^i, \tag{12}$$

where

$$\boldsymbol{v}_k^i = [x_k^{u_i} - r_k^i \cos b_k^i, \ y_k^{u_i} - r_k^i \cos b_k^i]^T \tag{13}$$

is the unbiased converted measurement error. The true range r_k^i and bearing b_k^i in (13) are unavailable in practice. It is thus necessary to compute the first two moments of $\boldsymbol{v}_k^i$ by an approximate approach that does not need the true range and bearing. Then the measurement-conditioned mean of $\boldsymbol{v}_k^i$ is given by [10]

$$\boldsymbol{\mu}_k^i = E[\boldsymbol{v}_k^i | r_k^{m_i}, b_k^{m_i}] = ((\lambda_1^i)^{-1} - \lambda_1^i) \begin{bmatrix} r_k^{m_i} \cos b_k^{m_i} \\ r_k^{m_i} \sin b_k^{m_i} \end{bmatrix} \tag{14}$$

and the corresponding covariance of $\boldsymbol{v}_k^i$ is given by

$$\boldsymbol{R}_k^i = \mathrm{cov}(\boldsymbol{v}_k^i | r_k^{m_i}, b_k^{m_i}), \tag{15}$$

where

$$\begin{aligned} \boldsymbol{R}_k^i(1,1) =& -(\lambda_1^i)^2 (r_k^{m_i})^2 \cos^2 b_k^{m_i} \\ &+ \frac{1}{2}((r_k^{m_i})^2 + \sigma_r^2)(1 + \lambda_4^i \cos 2b_k^{m_i}), \\ \boldsymbol{R}_k^i(2,2) =& -(\lambda_1^i)^2 (r_k^{m_i})^2 \sin^2 b_k^{m_i} \\ &+ \frac{1}{2}((r_k^{m_i})^2 + \sigma_r^2)(1 - \lambda_4^i \cos 2b_k^{m_i}), \\ \boldsymbol{R}_k^i(1,2) =& \boldsymbol{R}_k^i(2,1) = -(\lambda_1^i)^2 (r_k^{m_i})^2 \cos b_k^{m_i} \sin b_k^{m_i} \\ &+ \frac{1}{2}((r_k^{m_i})^2 + \sigma_r^2) \lambda_4^i \sin 2b_k^{m_i}. \end{aligned}$$

From (5), we have

$$\boldsymbol{x}(t_k^i) = \mathit{\Phi}^{-1}(t_k, t_k^i)(\boldsymbol{x}(t_k) - \boldsymbol{w}(t_k, t_k^i)). \tag{16}$$

Substituting (16) into (12), the i-th unbiased converted measurements during the time interval $(t_{k-1}, t_k]$ can then be rewritten as

$$\begin{aligned} \boldsymbol{y}_k^{u_i} &= \boldsymbol{H}_k^i \mathit{\Phi}^{-1}(t_k, t_k^i)(\boldsymbol{x}(t_k) - \boldsymbol{w}(t_k, t_k^i)) + \boldsymbol{v}_k^i \\ &= \boldsymbol{H}_k^i \mathit{\Phi}^{-1}(t_k, t_k^i)\boldsymbol{x}(t_k) - \boldsymbol{H}_k^i \mathit{\Phi}^{-1}(t_k, t_k^i)\boldsymbol{w}(t_k, t_k^i) + \boldsymbol{v}_k^i. \end{aligned} \tag{17}$$

Let

$$\begin{aligned} \bar{\boldsymbol{H}}_k^i &= \boldsymbol{H}_k^i \mathit{\Phi}^{-1}(t_k, t_k^i), \\ \bar{\boldsymbol{v}}_k^i &= \boldsymbol{v}_k^i - \bar{\boldsymbol{H}}_k^i \boldsymbol{w}(t_k, t_k^i). \end{aligned} \tag{18}$$

Then from (12), it follows that

$$\boldsymbol{y}_k^{u_i} = \bar{\boldsymbol{H}}_k^i \boldsymbol{x}(t_k) + \bar{\boldsymbol{v}}_k^i. \tag{19}$$

It can be easily seen from (5) and (12) that the mean and covariance of $\bar{\boldsymbol{v}}_k^i$ are

$$\begin{aligned} \bar{\boldsymbol{\mu}}_k^i &= \boldsymbol{\mu}_k^i, \\ \bar{\boldsymbol{R}}_k^i &= \boldsymbol{R}_k^i + \bar{\boldsymbol{H}}_k^i \boldsymbol{Q}(t_k, t_k^i)(\bar{\boldsymbol{H}}_k^i)^T \end{aligned} \tag{20}$$

and the auto-covariance of $\bar{\boldsymbol{v}}_k^i$ is

$$\mathrm{cov}(\bar{\boldsymbol{v}}_k^i, \bar{\boldsymbol{v}}_k^l) = \bar{\boldsymbol{H}}_k^i \boldsymbol{Q}(t_k, t_k^s)(\bar{\boldsymbol{H}}_k^l)^T, \ s = \max\{i, l\}. \tag{21}$$

By simply stacking all the unbiased converted measurements up during the time interval $(t_{k-1}, t_k]$, we have

$$\boldsymbol{y}_k^u = \boldsymbol{H}_k \boldsymbol{x}(t_k) + \boldsymbol{v}_k, \tag{22}$$

where

$$\begin{aligned} \boldsymbol{y}_k^u &= [(\boldsymbol{y}_k^{u_1})^T, (\boldsymbol{y}_k^{u_2})^T, \cdots, (\boldsymbol{y}_k^{u_{N_k}})^T]^T, \\ \boldsymbol{H}_k &= [(\bar{\boldsymbol{H}}_k^1)^T, (\bar{\boldsymbol{H}}_k^2)^T, \cdots, (\bar{\boldsymbol{H}}_k^{N_k})^T]^T, \\ \boldsymbol{v}_k &= [(\bar{\boldsymbol{v}}_k^1)^T, (\bar{\boldsymbol{v}}_k^2)^T, \cdots, (\bar{\boldsymbol{v}}_k^{N_k})^T]^T \end{aligned} \tag{23}$$

and the stacked measurement error $\boldsymbol{v}_k$ is still white with mean

$$\boldsymbol{\mu}_k = [(\bar{\boldsymbol{\mu}}_k^1)^T, (\bar{\boldsymbol{\mu}}_k^2)^T, \cdots, (\bar{\boldsymbol{\mu}}_k^{N_k})^T]^T \tag{24}$$

and covariance

$$\boldsymbol{R}_k = \begin{bmatrix} \boldsymbol{R}_k^1 + \bar{\boldsymbol{H}}_k^1 \boldsymbol{Q}(t_k, t_k^1)(\bar{\boldsymbol{H}}_k^1)^T & \cdots & \bar{\boldsymbol{H}}_k^1 \boldsymbol{Q}(t_k, t_k^{N_k})(\bar{\boldsymbol{H}}_k^{N_k})^T \\ \vdots & \ddots & \vdots \\ \bar{\boldsymbol{H}}_k^{N_k} \boldsymbol{Q}(t_k, t_k^{N_k})(\bar{\boldsymbol{H}}_k^1)^T & \cdots & \boldsymbol{R}_k^{N_k} + \bar{\boldsymbol{H}}_k^{N_k} \boldsymbol{Q}(t_k, t_k^{N_k})(\bar{\boldsymbol{H}}_k^{N_k})^T \end{bmatrix}. \tag{25}$$

In addition, the discrete-time process noise $\boldsymbol{w}(t_k, t_{k-1})$ of (5) is correlated with the measurement error $\boldsymbol{v}_k$ of (22). Thus the cross-covariance between $\boldsymbol{w}(t_k, t_{k-1})$ and $\boldsymbol{v}_k$ is

$$\begin{aligned} \boldsymbol{U}_k &= \mathrm{cov}(\boldsymbol{w}(t_k, t_{k-1}), \boldsymbol{v}_k) \\ &= [-\boldsymbol{Q}(t_k, t_k^1)(\bar{\boldsymbol{H}}_k^1)^T, \cdots, -\boldsymbol{Q}(t_k, t_k^{N_k})(\bar{\boldsymbol{H}}_k^{N_k})^T]^T. \end{aligned} \tag{26}$$

So far all the nonlinear measurements $\{\boldsymbol{z}_k^i\}_{i=1}^{N_k}$ obtained by asynchronous multi-rate radars during time interval $(t_{k-1}, t_k]$ have been converted into an augmented linear measurement $\boldsymbol{y}_k^u$ at time t_k. As a result, considering the discrete-time dynamic model (5), the original asynchronous nonlinear fusion problem has been transformed into a linear filtering problem. Assuming that the first two moments of $\boldsymbol{v}_k^i$ are known quantities in filtering, under the LMMSE estimation framework, the batch time-aligned asynchronous fusion with unbiased converted measurements can be easily obtained.

Let[1]

$$\begin{aligned} \boldsymbol{Y}_k^u &= [(\boldsymbol{y}_1^u)^T, (\boldsymbol{y}_2^u)^T, \cdots, (\boldsymbol{y}_k^u)^T]^T, \\ \hat{\boldsymbol{x}}_{k|k}^b &= E^*[\boldsymbol{x}(t_k) | \boldsymbol{Y}_k^u], \ \boldsymbol{P}_{k|k}^b = \mathrm{MSE}(\hat{\boldsymbol{x}}_{k|k}^b). \end{aligned} \tag{27}$$

[1] The LMMSE estimator of $\boldsymbol{x}$ given measurement $\boldsymbol{Y}$ (see [20, pp.123-128]) is denoted as $E^*[\boldsymbol{x}|\boldsymbol{Y}]$.

Theorem 1: Given the fused state estimate $\hat{\boldsymbol{x}}^b_{k-1|k-1}$ and its MSE matrix $\boldsymbol{P}^b_{k-1|k-1}$ at time t_{k-1}, the batch time-aligned asynchronous fusion with unbiased converted measurements at time t_k can be computed recursively by

$$\begin{aligned}\hat{\boldsymbol{x}}^b_{k|k} &= E^*[\boldsymbol{x}(t_k)|\boldsymbol{Y}^u_k] = \hat{\boldsymbol{x}}^b_{k|k-1} + \boldsymbol{K}^b_k(\boldsymbol{y}^u_k - \hat{\boldsymbol{y}}^u_{k|k-1}),\\ \boldsymbol{P}^b_{k|k} &= \mathrm{MSE}(\hat{\boldsymbol{x}}^b_{k|k}) = \boldsymbol{P}^b_{k|k-1} - \boldsymbol{K}^b_k\boldsymbol{S}^b_k(\boldsymbol{K}^b_k)^T,\end{aligned} \tag{28}$$

where

$$\begin{aligned}&\hat{\boldsymbol{x}}^b_{k|k-1} = \Phi(t_k,t_{k-1})\hat{\boldsymbol{x}}^b_{k-1|k-1},\\ &\boldsymbol{P}^b_{k|k-1} = \Phi(t_k,t_{k-1})\boldsymbol{P}^b_{k-1|k-1}\Phi^T(t_k,t_{k-1}) + \boldsymbol{Q}(t_k,t_{k-1}),\\ &\hat{\boldsymbol{y}}^u_{k|k-1} = \boldsymbol{H}_k\hat{\boldsymbol{x}}^b_{k|k-1} + \boldsymbol{\mu}_k,\\ &\boldsymbol{K}^b_k = \boldsymbol{C}^b_k(\boldsymbol{S}^b_k)^{-1},\\ &\boldsymbol{C}^b_k = \boldsymbol{P}^b_{k|k-1}\boldsymbol{H}^T_k + \boldsymbol{U}_k,\\ &\boldsymbol{S}^b_k = \boldsymbol{H}_k\boldsymbol{P}^b_{k|k-1}\boldsymbol{H}^T_k + \boldsymbol{R}_k + \boldsymbol{H}_k\boldsymbol{U}_k + \boldsymbol{U}^T_k\boldsymbol{H}^T_k.\end{aligned}$$

Proof: See Appendix A.

Note that the above batch asynchronous fusion algorithm is not optimal in the sense of LMMSE, although it adopts the LMMSE estimation framework. The error covariance (15) is computed conditioned on the measurements. This results in a correlation between the measurement error covariance and the measurement itself. In the batch asynchronous fusion algorithm, this correlation is neglected. Next, we will present an optimal LMMSE asynchronous fusion algorithm.

B. Sequential LMMSE Asynchronous Fusion with Converted Measurements

Converting the raw radar measurements into Cartesian coordinates yields

$$\begin{aligned}x^{m_i}_k &= (r^i_k + \tilde{r}^i_k)\cos(b^i_k + \tilde{b}^i_k) = x(t^i_k)\cos\tilde{b}^i_k - y(t^i_k)\sin\tilde{b}^i_k\\ &\quad + \tilde{r}^i_k\cos b^i_k\cos\tilde{b}^i_k - \tilde{r}^i_k\sin b^i_k\sin\tilde{b}^i_k,\\ y^{m_i}_k &= (r^i_k + \tilde{r}^i_k)\sin(b^i_k + \tilde{b}^i_k) = y(t^i_k)\cos\tilde{b}^i_k + x(t^i_k)\sin\tilde{b}^i_k\\ &\quad + \tilde{r}^i_k\sin b^i_k\cos\tilde{b}^i_k + \tilde{r}^i_k\cos b^i_k\sin\tilde{b}^i_k,\end{aligned} \tag{29}$$

where $i = 1, 2, \cdots, N_k$.

Let

$$\begin{aligned}\boldsymbol{y}^{m_i}_k &= [x^{m_i}_k, y^{m_i}_k]^T,\\ \boldsymbol{y}^m_k &= [(\boldsymbol{y}^{m_1}_k)^T, (\boldsymbol{y}^{m_2}_k)^T, \cdots, (\boldsymbol{y}^{m_{N_k}}_k)^T]^T,\\ \boldsymbol{Y}^m_k &= [(\boldsymbol{y}^m_1)^T, (\boldsymbol{y}^m_2)^T, \cdots, (\boldsymbol{y}^m_k)^T]^T,\\ \boldsymbol{Y}^i_k &= [(\boldsymbol{Y}^m_{k-1})^T, (\boldsymbol{y}^{m_1}_k)^T, \cdots, (\boldsymbol{y}^{m_i}_k)^T]^T.\end{aligned} \tag{30}$$

From (5), the state $\boldsymbol{x}(t_k)$ at time t_k can be represented as

$$\boldsymbol{x}(t_k) = \Phi(t_k, t^i_k)\boldsymbol{x}(t^i_k) + \boldsymbol{w}(t_k, t^i_k) \tag{31}$$

and

$$\boldsymbol{x}(t_k) = \Phi(t_k, t^{i-1}_k)\boldsymbol{x}(t^{i-1}_k) + \boldsymbol{w}(t_k, t^{i-1}_k). \tag{32}$$

Substituting (32) into (31), then it follows that

$$\begin{aligned}\boldsymbol{x}(t^i_k) &= \Phi^{-1}(t_k,t^i_k)\boldsymbol{x}(t_k) - \Phi^{-1}(t_k,t^i_k)\boldsymbol{w}(t_k,t^i_k)\\ &= \Phi^{-1}(t_k,t^i_k)\Phi(t_k,t^{i-1}_k)\boldsymbol{x}(t^{i-1}_k)\\ &\quad + \Phi^{-1}(t_k,t^i_k)\boldsymbol{w}(t_k,t^{i-1}_k) - \Phi^{-1}(t_k,t^i_k)\boldsymbol{w}(t_k,t^i_k).\end{aligned} \tag{33}$$

Without loss of generality, we define

$$\hat{\boldsymbol{x}}^i_{k|k} = E^*[\boldsymbol{x}(t^i_k)|\boldsymbol{Y}^i_k],\ \boldsymbol{P}^i_{k|k} = \mathrm{MSE}(\hat{\boldsymbol{x}}^i_{k|k}), \tag{34}$$

$$\hat{\boldsymbol{x}}^s_{k|k} = E^*[\boldsymbol{x}(t_k)|\boldsymbol{Y}^m_k],\ \boldsymbol{P}^s_{k|k} = \mathrm{MSE}(\hat{\boldsymbol{x}}_{k|k}). \tag{35}$$

It can be seen from (33) and (34) that the state estimate $\boldsymbol{x}^i_{k|k}$ at time t^i_k can be easily obtained if $\hat{\boldsymbol{x}}^{i-1}_{k|k}$ and $\boldsymbol{P}^{i-1}_{k|k}$ at time t^{i-1}_k are given. Then from (35), the fused estimate $\hat{\boldsymbol{x}}^s_{k|k}$ at time t_k can be obtained.

In view of this, we assume that the estimate $\hat{\boldsymbol{x}}^{i-1}_{k|k}$ and its MSE matrix $\boldsymbol{P}^{i-1}_{k|k}$ at time t^{i-1}_k are given. Then for system (33) and converted measurements (29), the LMMSE estimator $\hat{\boldsymbol{x}}^i_{k|k}$ of state $\boldsymbol{x}(t^i_k)$ is

$$\begin{aligned}\hat{\boldsymbol{x}}^i_{k|k} &= E^*[\boldsymbol{x}(t^i_k)|\boldsymbol{y}^{m_i}_k, \boldsymbol{Y}^{i-1}_k]\\ &= \hat{\boldsymbol{x}}^{i-}_{k|k} + \boldsymbol{K}^i_k(\boldsymbol{y}^{m_i}_k - \hat{\boldsymbol{y}}^{m_i}_{k|k}),\\ \boldsymbol{P}^i_{k|k} &= \mathrm{MSE}(\hat{\boldsymbol{x}}^i_{k|k}) = \boldsymbol{P}^{i-}_{k|k} - \boldsymbol{K}^i_k\boldsymbol{S}^i_k(\boldsymbol{K}^i_k)^T,\end{aligned} \tag{36}$$

where

$$\hat{\boldsymbol{x}}^{i-}_{k|k} = E^*[\boldsymbol{x}(t^i_k)|\boldsymbol{Y}^{i-1}_k] = \Phi^{-1}(t_k,t^i_k)\Phi(t_k,t^{i-1}_k)\hat{\boldsymbol{x}}^{i-1}_{k|k},$$

$$\begin{aligned}\boldsymbol{P}^{i-}_{k|k} &= \Phi^{-1}(t_k,t^i_k)\Phi(t_k,t^{i-1}_k)\boldsymbol{P}^{i-1}_{k|k}(\Phi^{-1}(t_k,t^i_k)\Phi(t_k,t^{i-1}_k))^T\\ &\quad + \Phi^{-1}(t_k,t^i_k)\boldsymbol{Q}(t_k,t^{i-1}_k)(\Phi^{-1}(t_k,t^i_k))^T\\ &\quad - \Phi^{-1}(t_k,t^i_k)\boldsymbol{Q}(t_k,t^i_k)(\Phi^{-1}(t_k,t^i_k))^T,\end{aligned}$$

$$\hat{\boldsymbol{y}}^{m_i}_{k|k} = E^*[\boldsymbol{y}^{m_i}_k|\boldsymbol{Y}^{i-1}_k] = \lambda^i_1[\hat{\boldsymbol{x}}^{i-}_{k|k}(1),\ \hat{\boldsymbol{x}}^{i-}_{k|k}(3)]^T,$$

$$\boldsymbol{K}^i_k = \boldsymbol{C}^i_k(\boldsymbol{S}^i_k)^{-1},$$

$$\begin{aligned}\boldsymbol{C}^i_k &= \mathrm{cov}((\boldsymbol{x}(t^i_k) - \hat{\boldsymbol{x}}^{i-}_{k|k}),\ (\boldsymbol{y}^{m_i}_{k|k} - \hat{\boldsymbol{y}}^{m_i}_{k|k}))\\ &= \lambda^i_1[\boldsymbol{P}^{i-}_{k|k}(:,1),\ \boldsymbol{P}^{i-}_{k|k}(:,3)]\end{aligned}$$

and

$$\boldsymbol{S}^i_k = \mathrm{cov}((\boldsymbol{y}^{m_i}_{k|k} - \hat{\boldsymbol{y}}^{m_i}_{k|k})), \tag{37}$$

$$\begin{aligned}\boldsymbol{S}^i_k(1,1) =& \lambda^i_2\boldsymbol{P}^{i-}_{k|k}(1,1) + \lambda^i_3\boldsymbol{P}^{i-}_{k|k}(3,3)\\ &+ (\lambda^i_2 - (\lambda^i_1)^2)E[(\hat{\boldsymbol{x}}^{i-}_{k|k}(1))^2] + \lambda^i_3E[(\hat{\boldsymbol{x}}^{i-}_{k|k}(3))^2]\\ &+ \lambda^i_2(\sigma^i_r)^2E[\cos^2 b^i_k] + \lambda^i_3(\sigma^i_r)^2E[\sin^2 b^i_k],\\ \boldsymbol{S}^i_k(2,2) =& \lambda^i_2\boldsymbol{P}^{i-}_{k|k}(3,3) + \lambda^i_3\boldsymbol{P}^{i-}_{k|k}(1,1)\\ &+ (\lambda^i_2 - (\lambda^i_1)^2)E[(\hat{\boldsymbol{x}}^{i-}_{k|k}(3))^2] + \lambda^i_3E[(\hat{\boldsymbol{x}}^{i-}_{k|k}(1))^2]\\ &+ \lambda^i_2(\sigma^i_r)^2E[\sin^2 b^i_k] + \lambda^i_3(\sigma^i_r)^2E[\cos^2 b^i_k],\\ \boldsymbol{S}^i_k(1,2) =& \boldsymbol{S}^i_k(2,1) = (\lambda^i_2 - \lambda^i_3)\boldsymbol{P}^{i-}_{k|k}(1,3)\\ &+ (\lambda^i_2 - (\lambda^i_1)^2 - \lambda^i_3)E[\hat{\boldsymbol{x}}^{i-}_{k|k}(1)\hat{\boldsymbol{x}}^{i-}_{k|k}(3)]\\ &+ (\sigma^i_r)^2(\lambda^i_2 - \lambda^i_3)E[\cos b^i_k\sin b^i_k].\end{aligned}$$

Note that $\hat{\boldsymbol{x}}^{i-}_{k|k}(i)$ stands for the i-th element of $\hat{\boldsymbol{x}}^{i-}_{k|k}$, and $\boldsymbol{P}^{i-}_{k|k}(:,i)$ stands for the i-th column vector of $\boldsymbol{P}^{i-}_{k|k}$.

At the fusion center, the prior estimate given at time t_k is $\hat{\boldsymbol{x}}^s_{k-1|k-1}$ rather than $\hat{\boldsymbol{x}}^{i-1}_{k|k}$, and the fused estimate needed is $\hat{\boldsymbol{x}}^s_{k|k}$. Using the LMMSE estimator (36), the remaining measurements during time interval $(t_{k-1}, t_k]$ can be fused similarly.

Considering all these N_k measurements collected according to time sequence $t_k^1 \leq t_k^2 \leq \cdots \leq t_k^{N_k}$ during the time interval $(t_{k-1}, t_k]$, we define

$$\begin{aligned} t_k^0 &= t_{k-1}, \\ \hat{\boldsymbol{x}}_{k|k}^0 &= \hat{\boldsymbol{x}}_{k-1|k-1}^s, \\ \boldsymbol{P}_{k|k}^0 &= \boldsymbol{P}_{k-1|k-1}^s. \end{aligned} \tag{38}$$

Then, given $\hat{\boldsymbol{x}}_{k-1|k-1}^s$ and $\boldsymbol{P}_{k-1|k-1}^s$ at time t_{k-1}, the sequential LMMSE asynchronous fusion with converted measurements at time t_k can be obtained.

Theorem 2: Given the fused state estimate $\hat{\boldsymbol{x}}_{k-1|k-1}^s$ and its MSE matrix $\boldsymbol{P}_{k-1|k-1}^s$ at time t_{k-1}, the sequential LMMSE asynchronous fusion with converted measurements at time t_k can be computed recursively as follows:

Starting from the prediction to t_k from t_{k-1},

$$t_k^0 = t_{k-1},\ \hat{\boldsymbol{x}}_{k|k}^0 = \hat{\boldsymbol{x}}_{k-1|k-1}^s,\ \boldsymbol{P}_{k|k}^0 = \boldsymbol{P}_{k-1|k-1}^s,$$

the sequential updates is repeated for $i = 1, 2, \cdots, N_k$,

$$\begin{aligned} \hat{\boldsymbol{x}}_{k|k}^{i-} &= \Phi^{-1}(t_k, t_k^i)\Phi(t_k, t_k^{i-1})\hat{\boldsymbol{x}}_{k|k}^{i-1}, \\ \boldsymbol{P}_{k|k}^{i-} &= \Phi(t_k^i, t_k^{i-1})\boldsymbol{P}_{k|k}^{i-1}\Phi^T(t_k^i, t_k^{i-1}) + \Phi^{-1}(t_k, t_k^i) \\ &\quad \times (\boldsymbol{Q}(t_k, t_k^{i-1}) - \boldsymbol{Q}(t_k, t_k^i))(\Phi^{-1}(t_k, t_k^i))^T, \\ \hat{\boldsymbol{y}}_{k|k}^{m_i} &= \lambda_1^i[\hat{\boldsymbol{x}}_{k|k}^{i-}(1),\ \hat{\boldsymbol{x}}_{k|k}^{i-}(3)]^T, \\ \boldsymbol{K}_k^i &= \boldsymbol{C}_k^i(\boldsymbol{S}_k^i)^{-1}, \\ \hat{\boldsymbol{x}}_{k|k}^i &= \hat{\boldsymbol{x}}_{k|k}^{i-} + \boldsymbol{K}_k^i(\boldsymbol{y}_k^{m_i} - \hat{\boldsymbol{y}}_{k|k}^{m_i}), \\ \boldsymbol{P}_{k|k}^i &= \boldsymbol{P}_{k|k}^{i-} - \boldsymbol{K}_k^i\boldsymbol{S}_k^i(\boldsymbol{K}_k^i)^T. \end{aligned}$$

Finally,

$$\begin{aligned} \hat{\boldsymbol{x}}_{k|k}^s &= \Phi(t_k, t_k^{N_k})\hat{\boldsymbol{x}}_{k|k}^{N_k}, \\ \boldsymbol{P}_{k|k}^s &= \Phi(t_k, t_k^{N_k})\boldsymbol{P}_{k|k}^{N_k}\Phi^T(t_k, t_k^{N_k}) + \boldsymbol{Q}(t_k, t_k^{N_k}). \end{aligned} \tag{39}$$

Proof: See Appendix B.

The above proposed sequential asynchronous fusion algorithm is optimal in the sense of minimizing the mean square error in the class of all linear estimators. Compared with the batch time-aligned asynchronous fusion algorithm that requires the first two moments of the unbiased converted measurement errors, the sequential LMMSE asynchronous fusion algorithm computes the predicted measurement error covariance $\boldsymbol{S}_k$ needed in filtering directly. When $t_{k-1} < t_k^1 = t_k^2 = \cdots = t_k^{N_k} = t_k$, the parallel filtering algorithm for LMMSE sequential synchronous fusion in [16] can be easily obtained because $\Phi(t_k, t_k^i) = \boldsymbol{I}$ and $\boldsymbol{Q}(t_k, t_k^i) = 0$ for $i = 1, \cdots, N_k$ in such a case.

IV. Illustrative Examples

Numerical examples are provided in this section to demonstrate the effectiveness of the proposed two asynchronous fusion algorithms with converted measurements. For comparison, the extensions of nonlinear filters using deterministic sampling, e.g., DDF in [5] and UKF in [4], available for asynchronous multi-radar tracking problem, are implemented in this numerical example. The raw radar measurement (3) is modeled by

$$\boldsymbol{z}_k^i = g(\boldsymbol{x}(t_k), \boldsymbol{w}(t_k, t_k^i)) + \boldsymbol{v}_k^i, \tag{40}$$

where

$$g(\boldsymbol{x}(t_k), \boldsymbol{w}(t_k, t_k^i)) = h(\Phi^{-1}(t_k, t_k^i)(\boldsymbol{x}(t_k) - \boldsymbol{w}(t_k, t_k^i)))$$

and $h(\cdot)$ is the nonlinear measurement function given by (4). Then similar to Theorem 1, by simply stacking all the measurements (40) up, the nonlinear filters using deterministic sampling with cross-correlated process and measurement noises at one time step apart can be applied.

We compare performance of the proposed batch time-aligned asynchronous fusion with unbiased converted measurements (BAF-UCM), the proposed sequential LMMSE asynchronous fusion (SLMMSEAF) with the batch time-aligned asynchronous fusion using the DDF and UKF (BAF-DDF, BAF-UKF). The performance evaluation matrices adopted are root mean squared error (RMSE), noncredibility index (NCI) [21], and inclination indicator (II) [21]. All results below are averaged over 500 Monte Carlo runs.

Consider the following continuous-time motion model of a target

$$\dot{\boldsymbol{x}}(t) = \boldsymbol{A}\boldsymbol{x}(t) + \boldsymbol{D}\widetilde{\boldsymbol{w}}(t), \quad \widetilde{\boldsymbol{w}}(t) \sim \mathcal{N}(0, \tilde{\boldsymbol{q}}(t)), \tag{41}$$

where

$$\boldsymbol{x} = [x, \dot{x}, y, \dot{y}]^T, \quad \boldsymbol{x}(0) \sim \mathcal{N}(\bar{\boldsymbol{x}}_0, \boldsymbol{P}_0).$$

The target motion is observed by three radars independently with sampling periods $T_1 = 0.5$s, $T_2 = 1$s, $T_1 = 1.2$s, and initial sampling time instants $t_1^0 = 0.2$s, $t_2^0 = 1$s, $t_3^0 = 0.6$s, respectively. Therefore they are multi-rate and asynchronous. The fusion center performs fusion operation with period $T_f = 1$s and initial time instant $t_f^0 = 1$s.

Two scenarios differing in target motion model and measurement accuracy are considered. In the first scenario, the target moves with a constant velocity (CV) motion model with

$$\boldsymbol{A} = \begin{bmatrix} 0 & 1 & 0 & 0 \\ 0 & 0 & 0 & 0 \\ 0 & 0 & 0 & 1 \\ 0 & 0 & 0 & 0 \end{bmatrix}, \quad \boldsymbol{D} = \begin{bmatrix} 0 & 0 \\ 1 & 0 \\ 0 & 0 \\ 0 & 1 \end{bmatrix}$$

and the standard deviations of range and bearing measurement errors of three radars are

$$\begin{aligned} \sigma_r^1 &= 500\text{m}, \quad \sigma_b^1 = 300\text{mrad}, \\ \sigma_r^2 &= 300\text{m}, \quad \sigma_b^2 = 200\text{mrad}, \\ \sigma_r^3 &= 200\text{m}, \quad \sigma_b^3 = 250\text{mrad} \end{aligned}$$

and all fusion algorithms are initialized with $\bar{\boldsymbol{x}}_0 = [-1000\text{m}, 50\text{m/s}, -1000\text{m}, 100\text{m/s}]^T$, $\boldsymbol{P}_0 = \text{diag}\left(10^5\text{m}^2, 10^3\text{m}^2/\text{s}^2, 10^5\text{m}^2, 10^3\text{m}^2/\text{s}^2\right)$.

Figs 2-5 shows comparison results for scenario 1. It can be seen that the proposed batch time-aligned asynchronous fusion with unbiased converted measurements outperforms the batch asynchronous fusion algorithms using DDF and UKF significantly both in position and velocity RMSEs. In terms of

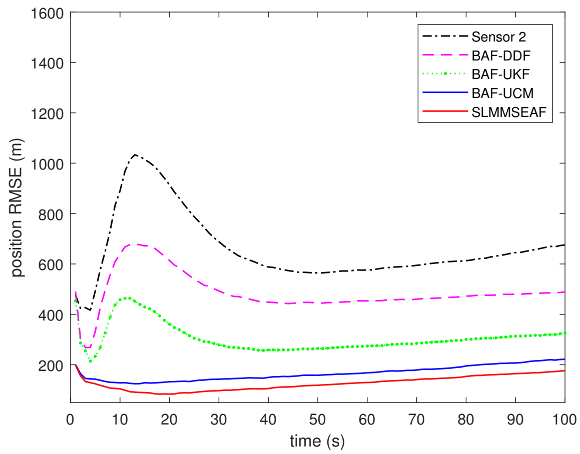

Fig. 2: Position RMSE (m) in scenario 1.

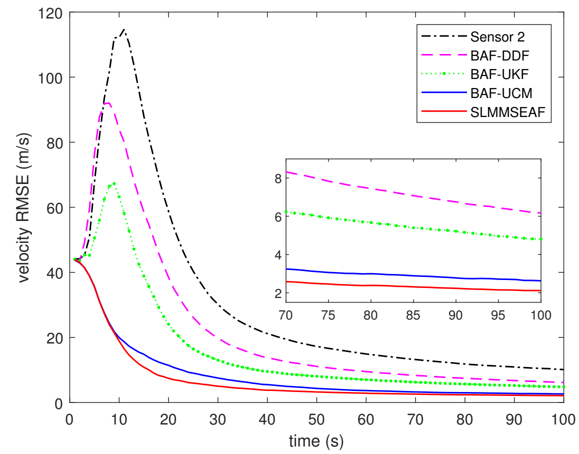

Fig. 3: Velocity RMSE (m/s) in scenario 1.

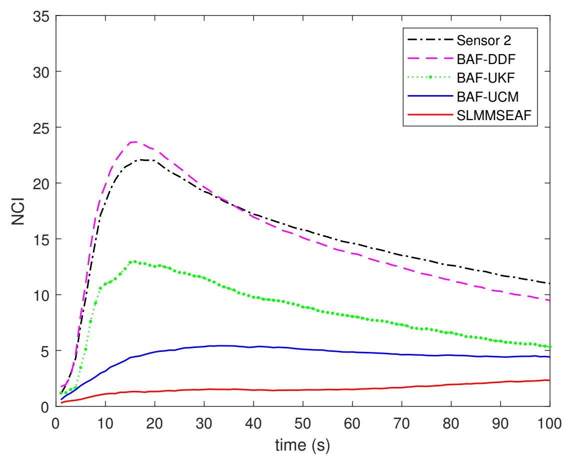

Fig. 4: NCI in scenario 1.

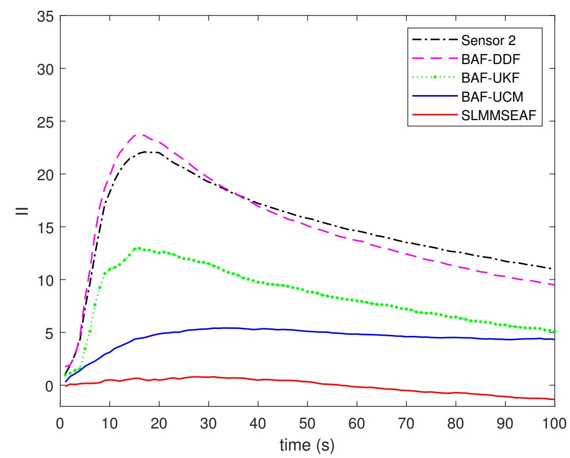

Fig. 5: II in scenario 1.

filter credibility, the batch asynchronous fusion with unbiased converted measurements is more credible than those using DDF and UKF. Moreover, the proposed sequential LMMSE asynchronous fusion algorithm has better performance than the batch asynchronous fusion with unbiased converted measurements no matter what metric is used for evaluation. The main reason is that the sequential LMMSE asynchronous fusion minimizes the mean square error among all linear estimators.

In the second scenario, the target moves with a constant turn (CT) motion model with

$$\boldsymbol{A} = \begin{bmatrix} 0 & 1 & 0 & 0 \\ 0 & 0 & 0 & -\omega \\ 0 & 0 & 0 & 1 \\ 0 & \omega & 0 & 0 \end{bmatrix}, \quad \boldsymbol{D} = \begin{bmatrix} 0 & 0 \\ 1 & 0 \\ 0 & 0 \\ 0 & 1 \end{bmatrix}, \quad \omega = -3^{\mathrm{o}}/\mathrm{s}$$

and the standard deviations of range and bearing measurement errors of three radars are

$$\begin{aligned} \sigma_r^1 &= 250\mathrm{m}, \quad \sigma_b^1 = 200\mathrm{mrad}, \\ \sigma_r^2 &= 220\mathrm{m}, \quad \sigma_b^2 = 180\mathrm{mrad}, \\ \sigma_r^3 &= 150\mathrm{m}, \quad \sigma_b^3 = 150\mathrm{mrad} \end{aligned}$$

and all fusion algorithms are initialized with $\bar{\boldsymbol{x}}_0 = [-1000\mathrm{m}, 50\mathrm{m/s}, -800\mathrm{m}, 80\mathrm{m/s}]^T$, $\boldsymbol{P}_0 = \mathrm{diag}\left(10^5\mathrm{m}^2, 10^3\mathrm{m}^2/\mathrm{s}^2, 10^5\mathrm{m}^2, 10^3\mathrm{m}^2/\mathrm{s}^2\right)$.

As shown in Figs. 6-9 for scenario 2, the proposed batch time-aligned asynchronous fusion with unbiased converted measurements has better performance than the batch asynchronous fusion using DDF and UKF significantly in terms of both estimation accuracy and filter credibility. As expected, the proposed sequential LMMSE asynchronous fusion algorithm performs the best no matter what metric is used for comparison. This also demonstrates the effectiveness of the sequential LMMSE asynchronous fusion with converted measurements and the batch time-aligned asynchronous fusion with unbiased converted measurements.

V. Conclusions

In this paper, the problem of target tracking with asynchronous multi-rate multi-radar measurements is investigated. Two asynchronous fusion algorithms are proposed using converted measurements. By aligning measurements collected at different time instants to a common fusion time instant, a batch

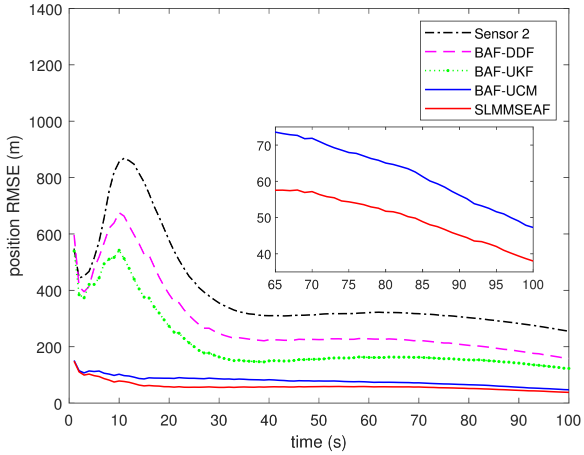

Fig. 6: Position RMSE (m) in scenario 2.

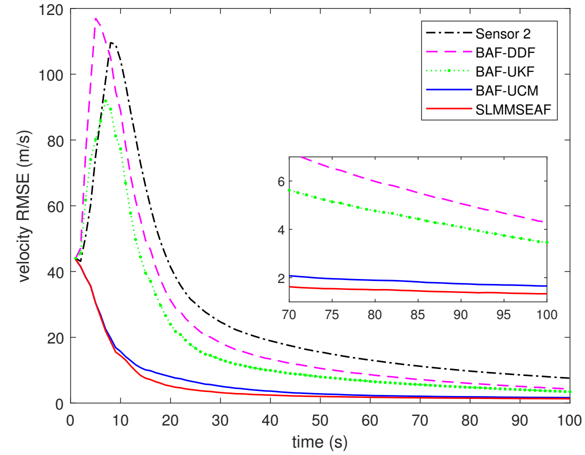

Fig. 7: Velocity RMSE (m/s) in scenario 2.

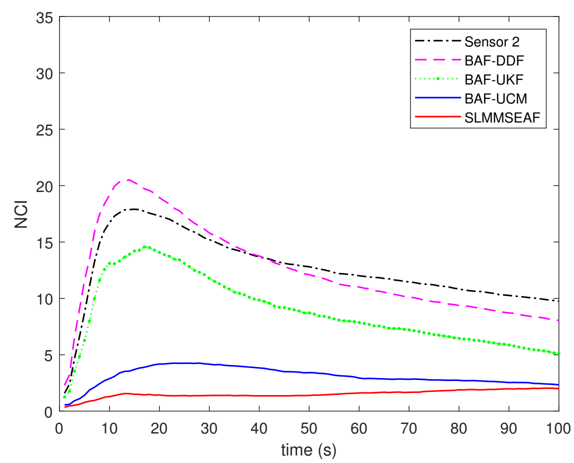

Fig. 8: NCI in scenario 2.

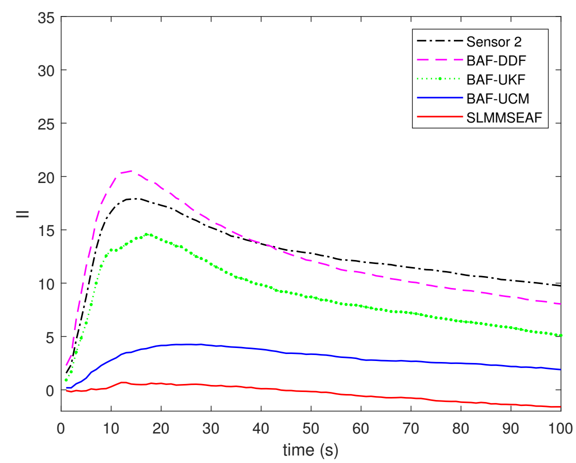

Fig. 9: II in scenario 2.

time-aligned asynchronous fusion algorithm is developed. By constructing a state-transition model to the measurement time instant according to the discretized continuous-time target dynamics, a sequential LMMSE asynchronous fusion algorithm is developed, which is optimal in the sense of minimizing the mean square error among all linear estimators. During the sampling period of the fusion center, the former performs the tracking operation in a batch manner, and the latter performs the tracking operation in a sequential manner. They are both centralized fusion algorithms. Numerical examples have shown that in terms of accuracy and credibility the proposed two asynchronous fusion with converted measurements are both preferred.

Appendix A
Proof of Theorem 1

Given $\hat{\boldsymbol{x}}^b_{k-1|k-1}$ and $\boldsymbol{P}^b_{k-1|k-1}$ at time t_{k-1}, the predicted state and its MSE matrix are

$$\hat{\boldsymbol{x}}^b_{k|k-1} = E^*[\boldsymbol{x}(t_k)|\boldsymbol{Y}^u_{k-1}] = \Phi(t_k, t_{k-1})\hat{\boldsymbol{x}}^b_{k-1|k-1},$$

$$\boldsymbol{P}^b_{k|k-1} = E[(\boldsymbol{x}(t_k) - \hat{\boldsymbol{x}}^b_{k|k-1})(\boldsymbol{x}(t_k) - \hat{\boldsymbol{x}}^b_{k|k-1})^T].$$

The predicted measurement is

$$\begin{aligned}\hat{\boldsymbol{y}}^u_{k|k-1} &= E^*[\boldsymbol{y}^u_k|\boldsymbol{Y}^u_{k-1}] = \boldsymbol{H}_k E^*[\boldsymbol{x}(t_k)|\boldsymbol{Y}^u_{k-1}] + E^*[\boldsymbol{v}_k|\boldsymbol{Y}^u_{k-1}] \\ &= \boldsymbol{H}_k \hat{\boldsymbol{x}}^b_{k|k-1} + \boldsymbol{\mu}_k.\end{aligned}$$

The predicted measurement error covariance is

$$\begin{aligned}\boldsymbol{S}^b_k &= E[(\boldsymbol{y}^u_k - \hat{\boldsymbol{y}}^u_{k|k-1})(\boldsymbol{y}^u_k - \hat{\boldsymbol{y}}^u_{k|k-1})^T] \\ &= E[(\boldsymbol{H}_k(\boldsymbol{x}(t_k) - \hat{\boldsymbol{x}}^b_{k|k-1}) + (\boldsymbol{v}_k - \boldsymbol{\mu}_k))(\cdot)^T] \\ &= \boldsymbol{H}_k E[(\boldsymbol{x}(t_k) - \hat{\boldsymbol{x}}^b_{k|k-1})(\cdot)^T]\boldsymbol{H}^T_k + E[(\boldsymbol{v}_k - \boldsymbol{\mu}_k)(\cdot)^T] \\ &\quad + E[(\boldsymbol{x}(t_k) - \hat{\boldsymbol{x}}^b_{k|k-1})(\boldsymbol{v}_k - \boldsymbol{\mu}_k)^T] \\ &\quad + E[(\boldsymbol{v}_k - \boldsymbol{\mu}_k)(\boldsymbol{x}(t_k) - \hat{\boldsymbol{x}}^b_{k|k-1})^T]\boldsymbol{H}^T_k \\ &= \boldsymbol{H}_k \boldsymbol{P}^b_{k|k-1}\boldsymbol{H}^T_k + \boldsymbol{R}_k + \boldsymbol{H}_k\boldsymbol{U}_k + \boldsymbol{U}^T_k\boldsymbol{H}^T_k,\end{aligned}$$

where $(\cdot)$ means the term right before it, and

$$\begin{aligned}&E[(\boldsymbol{x}(t_k) - \hat{\boldsymbol{x}}^b_{k|k-1})(\boldsymbol{v}_k - \boldsymbol{\mu}_k)^T] \\ &\quad = E[\boldsymbol{w}(t_k, t_{k-1})(\boldsymbol{v}_k - \boldsymbol{\mu}_k)^T] = \boldsymbol{U}_k.\end{aligned}$$

The cross-covariance is

$$\begin{aligned}\boldsymbol{C}_k^b &= E[(\boldsymbol{x}(t_k)-\hat{\boldsymbol{x}}_{k|k-1}^b)(\boldsymbol{y}_k^u-\hat{\boldsymbol{y}}_{k|k-1}^u)^T]\\ &= E[(\boldsymbol{x}(t_k)-\hat{\boldsymbol{x}}_{k|k-1}^b)(\boldsymbol{x}(t_k)-\hat{\boldsymbol{x}}_{k|k-1}^b)^T]\boldsymbol{H}_k^T\\ &\quad + E[(\boldsymbol{x}(t_k)-\hat{\boldsymbol{x}}_{k|k-1}^b)(\boldsymbol{v}_k-\boldsymbol{\mu}_k)^T]\\ &= \boldsymbol{P}_{k|k-1}^b\boldsymbol{H}_k^T+\boldsymbol{U}_k.\end{aligned}$$

This completes the proof of Theorem 1.

Appendix B
Proof of Theorem 2

The sequential LMMSE asynchronous fusion from t_k^{i-1} to t_k^i, $i=1,2,\cdots,N_k$, has been given by (36).

From (31) the state $\boldsymbol{x}(t_k^1)$ at time t_k^1 can be rewritten as

$$\boldsymbol{x}(t_k^1)=\varPhi^{-1}(t_k,t_k^1)\boldsymbol{x}(t_k)-\varPhi^{-1}(t_k,t_k^1)\boldsymbol{w}(t_k,t_k^1). \tag{42}$$

Substituting (5) into (42), then it follows that

$$\begin{aligned}\boldsymbol{x}(t_k^1)&=\varPhi^{-1}(t_k,t_k^1)\varPhi(t_k,t_{k-1})\boldsymbol{x}(t_{k-1})\\ &\quad+\varPhi^{-1}(t_k,t_k^1)\boldsymbol{w}(t_k,t_{k-1})-\varPhi^{-1}(t_k,t_k^1)\boldsymbol{w}(t_k,t_k^1).\end{aligned} \tag{43}$$

Let $t_k^0=t_{k-1}$. Then the above equation (43) becomes

$$\begin{aligned}\boldsymbol{x}(t_k^1)&=\varPhi^{-1}(t_k,t_k^1)\varPhi(t_k,t_k^0)\boldsymbol{x}(t_k^0)\\ &\quad+\varPhi^{-1}(t_k,t_k^1)\boldsymbol{w}(t_k,t_k^0)-\varPhi^{-1}(t_k,t_k^1)\boldsymbol{w}(t_k,t_k^1).\end{aligned}$$

This is consistent with the discrete-time system (33) for $i=1$.

For the final update $\hat{\boldsymbol{x}}_{k|k}^s$, given $\boldsymbol{x}(t_k^{N_k})$ and $\boldsymbol{P}_{k|k}^{N_k}$, we have

$$\begin{aligned}\hat{\boldsymbol{x}}_{k|k}^s&=E^*[\boldsymbol{x}(t_k)|\boldsymbol{Y}_k^m]=\varPhi(t_k,t_k^{N_k})E^*[\boldsymbol{x}(t_k^{N_k})|\boldsymbol{Y}_k^m]\\ &=\varPhi(t_k,t_k^{N_k})\hat{\boldsymbol{x}}_{k|k}^{N_k}\end{aligned}$$

and its MSE matrix is

$$\begin{aligned}\boldsymbol{P}_{k|k}^s&=E[(\boldsymbol{x}(t_k)-\hat{\boldsymbol{x}}_{k|k}^s)(\boldsymbol{x}(t_k)-\hat{\boldsymbol{x}}_{k|k}^s)^T]\\ &=\varPhi(t_k,t_k^{N_k})E[(\boldsymbol{x}(t_k^{N_k})-\hat{\boldsymbol{x}}_{k|k}^{N_k})(\cdot)^T]\varPhi^T(t_k,t_k^{N_k})\\ &\quad+E[\boldsymbol{w}(t_k,t_k^{N_k})\boldsymbol{w}^T(t_k,t_k^{N_k})]\\ &=\varPhi(t_k,t_k^{N_k})\boldsymbol{P}_{k|k}^{N_k}\varPhi^T(t_k,t_k^{N_k})+\boldsymbol{Q}(t_k,t_k^{N_k}).\end{aligned}$$

Note that if $t_k^{N_k}=t_k$, $\varPhi(t_k,t_k^{N_k})=\boldsymbol{I}$, $\boldsymbol{Q}(t_k,t_k^{N_k})=0$, then it follows that

$$\hat{\boldsymbol{x}}_{k|k}^s=\hat{\boldsymbol{x}}_{k|k}^{N_k},\ \boldsymbol{P}_{k|k}^s=\boldsymbol{P}_{k|k}^{N_k}.$$

This completes the proof of Theorem 2.

References

[1] S. Bordonaro, P. Willett, and Y. Bar-Shalom, “Consistent linear tracker with converted range, bearing, and range rate measurements,” *IEEE Transactions on Aerospace and Electronic Systems*, vol. 53, no. 6, pp. 3135–3149, 2017.

[2] L. P. Yan, C. Y. Di, Q. M. J. Wu, and Y. Xia, “Sequential fusion for multirate multisensor systems with heavy-tailed noises and unreliable measurements,” *IEEE Transactions on Systems, Man, and Cybernetics: Systems*, vol. 52, no. 1, pp. 523–532, 2022.

[3] R. Mehra, “A comparison of several nonlinear filters for reentry vehicle tracking,” *IEEE Transactions on Automatic Control*, vol. 16, no. 4, pp. 307–319, 1971.

[4] S. Julier, J. Uhlmann, and H. F. Durrant-Whyte, “A new method for the nonlinear transformation of means and covariances in filters and estimators,” *IEEE Transactions on Automatic Control*, vol. 45, no. 3, pp. 477–482, 2000.

[5] M. Norgaard, N. K. Poulsen, and O. Ravn, “New developments in state estimation for nonlinear systems,” *Automatica*, vol. 36, no. 11, pp. 1627–1638, 2000.

[6] P. Closas, C. Fernandez-Prades, and J. Vila-Valls, “Multiple quadrature Kalman filtering,” *IEEE Transactions on Signal Processing*, vol. 60, no. 12, pp. 6125–6137, 2012.

[7] M. S. Arulampalam, S. Maskell, N. J. Gordon, and T. Clapp, “A tutorial on particle filters for online nonlinear/non-gaussian bayesian tracking,” *IEEE Transactions on Signal Processing*, vol. 50, no. 2, pp. 174–188, 2002.

[8] D. Lerro and Y. Bar-Shalom, “Tracking with debiased consistent converted measurements versus EKF,” *IEEE Transactions on Aerospace and Electronic Systems*, vol. 29, no. 3, pp. 1015–1022, 1993.

[9] L. Mo, X. Song, Y. Zhou, Z. Sun, and Y. Bar-Shalom, “Unbiased converted measurements for tracking,” *IEEE Transactions on Aerospace and Electronic Systems*, vol. 34, no. 3, pp. 1023–1027, 1998.

[10] Z. S. Duan, C. Z. Han, and X. R. Li, “Comments on ”unbiased converted measurements for tracking”,” *IEEE Transactions on Aerospace and Electronic Systems*, vol. 40, no. 4, pp. 1374–1377, 2004.

[11] S. Bordonaro, P. Willett, and Y. Bar-Shalom, “Decorrelated unbiased converted measurement Kalman filter,” *IEEE Transactions on Aerospace and Electronic Systems*, vol. 50, no. 2, pp. 1431–1444, 2014.

[12] S. J. Julier and J. K. Uhlmann, “Consistent debiased method for converting between polar and cartesian coordinate systems,” in *Proceedings of Acquisition, Tracking, and Pointing XI*, Orlando, Florida, USA, October, 1997.

[13] Z. L. Zhao, X. R. Li, and V. P. Jilkov, “Best linear unbiased filtering with nonlinear measurements for target tracking,” *IEEE Transactions on Aerospace and Electronic Systems*, vol. 40, no. 4, pp. 1324–1336, 2004.

[14] Z. S. Duan, Y. M. Wang, and X. R. Li, “Recursive LMMSE centralized fusion with recombination of multi-radar measurements,” in *Proceedings of 2011 International Conference on Information Fusion*, Chicago, IL, July 5-8, 2011.

[15] Q. P. Zhang, Z. S. Duan, and U. D. Hanebeck, “Recursive LMMSE centralized fusion with compressed multi-radar measurements,” in *Proceedings of 2019 International Conference on Control, Automation and Information Sciences*, Chengdu, China, October 23-26, 2019.

[16] D. L. Zhang and Z. S. Duan, “Recursive LMMSE sequential fusion with multi-radar measurements for target tracking,” in *Proceedings of 2021 International Conference on Information Fusion*, Sun City, South Africa, November 1-4, 2021.

[17] Y. Y. Hu, Z. S. Duan, and D. H. Zhou, “Estimation fusion with general asynchronous multi-rate sensors,” *IEEE Transactions on Aerospace and Electronic Systems*, vol. 46, no. 4, pp. 2090–2102, 2010.

[18] D. Jeon and Y. Eun, “Distributed asynchronous multiple sensor fusion with nonlinear multiple models,” *Aerospace Science and Technology*, vol. 39, pp. 692–704, 2014.

[19] J. K. Yan, H. W. Liu, W. Q. Pu, and Z. Bao, “Decentralized 3-D target tracking in asynchronous 2-D radar network: Algorithm and performance evaluation,” *IEEE Sensors Journal*, vol. 17, no. 3, pp. 823–833, 2017.

[20] Y. Bar-Shalom, X. R. Li, and T. Kirubarajan, *Estimation with Applications to Tracking and Navigation*. New York: John Wiley & Sons, 2001.

[21] X. R. Li and Z. L. Zhao, “Measuring estimator’s credibility: Noncredibility index,” in *Proceedings of 2006 International Conference on Information Fusion*, Florence, Italy, July 2006.